Rhenium Inhibitors of Cathepsin B (ReO(SYS)X (Where Y = S, py; X = Cl, Br, SPhOMe-*p*)): Synthesis and Mechanism of Inhibition

Renee Mosi, Ian R. Baird,* Jennifer Cox, Virginia Anastassov, Beth Cameron, Renato T. Skerlj, and Simon P. Fricker

AnorMED Inc., Suite 200, 20353 64th Avenue, Langley BC V2Y1N5, Canada

Received March 27, 2006

The synthesis of four new oxorhenium(V) complexes containing the "3 + 1" mixed-ligand donor set, ReO(SYS)X (where Y = S, py; X = Cl, Br), is described. All of the complexes tested exhibited selectivity for cathepsin B over K. Most notably, compound **6**, ReO(SSS-2,2′)Br (IC_{50}(cathepsin B) = 1.0 nM), was 260 times more potent against cathepsin B. It was also discovered that complexes containing the same tridentate (SSS) ligand were more potent when the leaving group was bromide versus chloride (e.g., IC_{50}(cathepsin B): ReO(SSS-2,2′)Cl (**4**), 8.8 nM; ReO(SSS-2,2′)Br (**6**), 1.0 nM). Mechanistic studies with cathepsin B showed that both compounds **2** (ReO(SpyS)(SPhOMe-*p*)) and **4** were active-site-directed. Compound **2** was determined to be a tight-binding, reversible inhibitor, while compound **4** was a time-dependent, slowly reversible inhibitor. The results described in this paper show that the oxorhenium(V) "3 + 1" complexes are potent, selective inhibitors of cathepsin B and have potential for the treatment of cancer.

1. Introduction

Protease enzymes catalyze the cleavage of proteins and can be divided into five mechanistic classes defined by the functional amino acid residue at the active site. These protease classes are the serine, aspartate, cysteine, metallo, and threonine proteases. An imbalance in the regulation of protease activity can contribute to a number of disease processes, and the cysteine proteases have been implicated in the pathophysiology of several diseases including inflammatory airway diseases, bone and joint disorders, parasitic diseases, and cancer.[1−6] The most extensively studied lysosomal cysteine protease, cathepsin B, is of particular interest in our laboratory for its role in cancer.

Cathepsin B is capable of degrading components of the extracellular matrix in such diseases as muscular dystrophy,[7] rheumatoid arthritis,[8] and tumor invasiveness.[9] With respect to the last, cathepsin B has been demonstrated to be a prognostic marker for several types of cancer (colorectal,[10] prostate,[11] gastric,[12] pancreatic,[13] non-small-cell lung,[14] breast,[15] and brain[16]). Increased expression and secretion of cathepsin B have been shown to be associated with numerous human and experimental tumors.[17−20] The exact role for cathepsin B in solid tumors has yet to be defined, but it has been proposed to be involved in metastasis, angiogenesis, and tumor progression.[21−24] Carcinoma cell invasion and metastasis can be inhibited by the nonspecific, irreversible, cysteine protease inhibitor E-64.[25−27,a] Cathepsin B therefore presents itself as a possible therapeutic target for the control of tumor progression.

The cysteine protease active site is composed of cysteine, histidine, and asparagine residues in a catalytic triad. The cysteine and histidine form a stable thiolate−imidazolium ion pair, which is essential for enzyme activity. Scheme 1 illustrates the nucleophilic attack of the thiolate cysteine on the carbonyl carbon of the substrate, resulting in a tetrahedral intermediate. A covalent-bound acyl enzyme is formed upon cleavage of the peptide bond. Hydrolysis of the acyl enzyme allows the regeneration of the free enzyme. The majority of cysteine protease inhibitors form either a reversible or irreversible covalent bond with the reactive cysteine in the active site, thereby blocking the proteolytic activity of the enzyme.[28] Several such inhibitors have been synthesized, and mechanistic studies have ensued.

Scheme 1

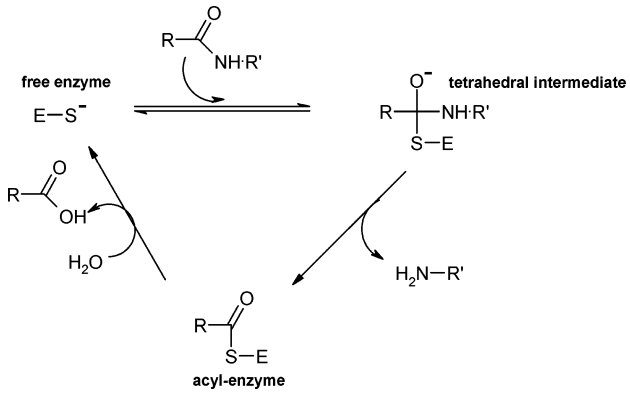

Chymostatin and leupeptin (naturally occurring compounds produced by certain *Streptomyces* strains) both contain peptide sequences, which serve to bind the inhibitor in the active site,[29] along with a reactive amino acid aldehyde, which reacts reversibly with the active-site cysteine to form a tetrahedral hemithioacetal.[30] The peptidyl aldehydes are slow-binding inhibitors of cathepsin B.[31] E-64, isolated from *Aspergillus japonicus*,[32] was shown to be a general inhibitor for the entire family of cathepsins with no selectivity for one over the other.[33] Incorporation of the epoxysuccinyl group of E-64 (the point of reaction by the nucleophilic cysteine residue) into peptides with slightly modified structures compared to that of E-64 yielded the cathepsin B-specific inhibitors CA030 and CA074. The X-ray crystal analysis of cathepsin B inhibited by both CA030[34] and CA074[35] has been reported, and more recently the crystal structure of the epoxysuccinyl inhibitor NS-134, specific for cathepsin B, was reported.[36] Another novel class of cathepsin B inhibitors uses the heterocycle 1,2,4-thiadiazole as the thiol trapping pharmacophore.[37,38]

* To whom correspondence should be addressed. Phone: (604) 530-1057. Fax: (604) 530-0976. E-mail:ibaird@anormed.com.

[a] Abbreviations: AMC, aminomethylcoumarin; DTT, dithiothreitol; E-64, L-*trans*-epoxysuccinylleucylamido(4-guanidino)butane; pNA, *p*-nitroaniline; RFU, relative fluorescence units.

10.1021/jm060357z CCC: $33.50
Published on Web 07/27/2006

Scheme 2

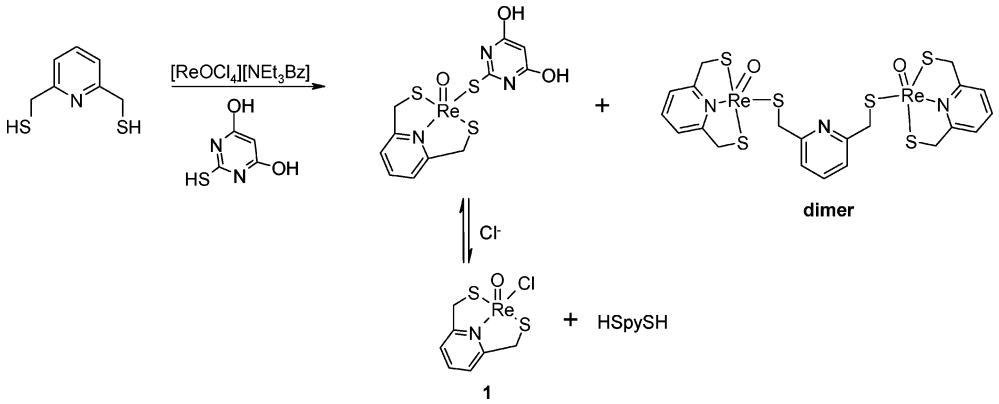

Cathepsin B is unique among the papain family of cysteine proteases because it has endopeptidase activity (cleaves proteins in the middle of the molecule) and has dipeptidyl exopeptidase activity (cleaves two amino acid units from the C-terminus end of proteins).[39] This activity is due to a unique structural feature known as the occluding loop,[40] which partially blocks the active site. The basic residues His110 and His111 are located in this loop in such a way as to be well placed to interact with the free C-terminal carboxylate of a polypeptide chain, directing it into position for hydrolysis of the C-terminal dipeptide. The occluding loop provides structural constraints for the design of an inhibitor, which will be able to functionally access the active-site cysteine.

We have developed a program to investigate metal-based compounds as potential inhibitors of cysteine proteases. Several different metal-based compounds (containing Ru, Ni, Pd, Au, and Re in several different oxidation states) have been investigated in our laboratory, and the most potent compounds are those containing the oxorhenium(V) core using the "3 + 1" mixed-ligand donor set. The major advantage of using the "3 + 1" mixed-ligand complex concept is that it allows for the preparation of an array of compounds by modifying either the chelating tridentate ligand or the monodentate ligand.[41−45] The rhenium center is very sulfurphilic, and others have proposed that the rhenium center forms a covalent Re−S bond with the cysteine in the active site to give a reversible rhenium-bound inhibitor;[46,47] however, the reversibility of this interaction was only speculated. The report that oxorhenium(V) "3 + 1" complexes undergo a reversible reaction with nonprotein thiol-containing molecules such as glutathione and free cysteine in vivo further suggests their usefulness as potential reversible inhibitors against cathepsin B.[46−48] Recently we reported that oxorhenium(V) complexes containing the "3 + 1" mixed-ligand donor set, ReO(SXS)(SR) (where X = S, O, N(R′); R = alkyl, aryl, heterocycle; R′ = H, alkyl, aryl), were able to inhibit cathepsin B, with the most potent inhibitor, ReO(SSS)(S-4py)·HCl, exhibiting an IC_{50} of 10 nM.[49]

Reversibility of cathepsin B inhibition is a desirable property for therapeutic applications. Many enzymes contain cysteine active sites, and therefore, the possibility of cross-reactivity is strong. The in vivo consequences of irreversibly inactivating nontarget enzymes could lead to serious side effects. We have employed several techniques to investigate the reversibility of this interaction with the cysteine residue of cathepsin B. The data presented within will focus on this interaction, and its reversibility, between cathepsin B and several oxorhenium(V) complexes.

2. Results and Discussion

2.1. Synthesis. During the attempted synthesis of ReO(SpyS)(L_1) (where L_1 = 4,6-dihydroxy-2-mercaptopyrimidine or 4,6-diamino-2-mercaptopyrimidine) two products were isolated, neither being the desired complex. The major product was a very insoluble tan solid, which was determined to be the dimer $[ReO(SpyS)]_2(SpyS)$ by ^{1}H NMR and ESMS, while the minor product was a green solid determined to be compound **1** (ReO(SpyS)Cl; 10−12%). In an effort to increase the yield of **1,** $[BzEt_3N][ReOCl_4]$ was treated with 10 equiv of LiCl in MeOH followed by the addition of HSpySH; however, the major product was once again the dimer with approximately 3% of **1** isolated. The analogous reaction with $BzEt_3NCl$ also yielded predominantly $[ReO(SpyS)]_2(SpyS)$ dimer. This suggested that a higher chloride concentration would not block dimer formation and that the monodentate ligand (L_1) is essential for the formation of **1**; presumably ReO(SpyS)(L_1) is formed in situ and then is slowly converted to **1** via reaction with the free Cl^- in solution (Scheme 2). The finding that stirring the reaction mixture for 18 h, instead of the typical 2−3 h, gave **1** in 31% yield supports this hypothesis. Unfortunately, the yield of **1** could not be increased significantly with the addition of excess chloride after 3 h (i.e., once ReO(SpyS)(L_1) had formed in situ).

The monochloro and monobromo complexes were synthesized to investigate the effect that the chelate ring size would have on the activity of the rhenium complex against cathepsin B, presumably through nucleophilic displacement of the halide by the cysteine thiolate in the active site. Treatment of $[BzEt_3N][ReOCl_4]$ with HSSSH-2,2′ yields the air-stable compound **4** (ReO(SSS-2,2′)Cl), which has been used as a synthetic precursor for the synthesis of many oxorhenium(V) "3 + 1" complexes of composition ReO(SSS-2,2′)(SR) (Scheme 3). It should be noted that several groups, including ourselves, have tried to isolate the complexes ReO(SOS)Cl and ReO(SN(R)S)Cl with little success.[50] The thioether S atom forms a stronger interaction with the rhenium center than O and/or N(R), resulting in a stable complex.[51]

The HSSSH-2,3′ ligand was synthesized from commercially available 3-mercaptopropanol in four steps (overall yield of 19%). Addition of HSSSH-2,3′ to a solution of $[BzEt_3N][ReOBr_4]$ in methylene chloride gave compound **7** (ReO(SSS-2,3′)Br) in 14% yield (Scheme 3). The yield was quite low because the isolated precipitate needed to be washed with cold methylene chloride (partially soluble) several times to yield a product that had an HPLC purity greater than 90%. When $[BzEt_3N][ReOCl_4]$ was treated with HSSSH-2,3′ under similar conditions, the analogous chloride complex could not be isolated. A ^{1}H NMR spectrum of the crude reaction mixture

Scheme 3

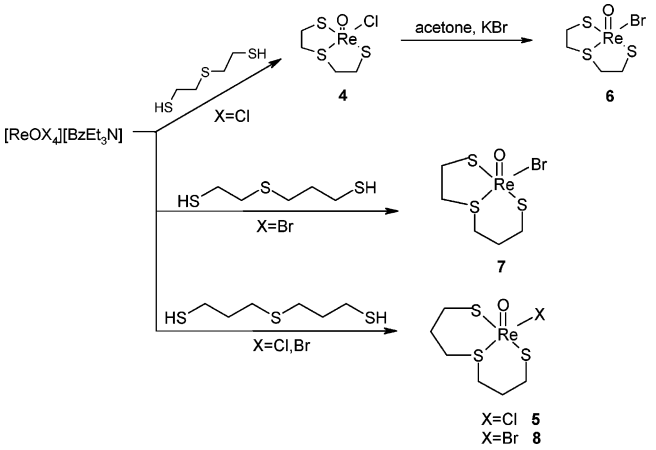

suggested ReO(SSS-2,3′)Cl was present (~10% by integration); however, several attempts to isolate and/or purify the desired complex were unsuccessful.

The HSSSH-3,3′ ligand was synthesized from commercially available 3,3′-thiodipropanol in three steps (overall yield of 42%). Addition of HSSSH-3,3′ to a solution of $[BzEt_3N][ReOCl_4]$ in methanol or $[BzEt_3N][ReOBr_4]$ in methylene chloride gave **5** (ReO(SSS-3,3′)Cl, 14%) or **8** (ReO(SSS-3,3′)-Br, 20%), respectively (Scheme 3). Once again, the yields are quite low and the isolated precipitates need to be washed with cold methylene chloride to ensure adequate purity.

2.2. SAR of Rhenium Complexes. The inhibition of several rhenium complexes against cathepsins B and K was evaluated in our laboratory with the goal of determining their activity and whether they show specificity for one enzyme over the other. One major advance in this regard has been the decreased reliance on high concentrations of thiols to maintain enzyme activity. Instead, we have found that the cysteine proteases can maintain good catalytic activity in the presence of low concentrations of thiols. Because many potential inhibitors contain thiol reactive groups, high concentrations of thiols in the assay mixture would limit the study of the interaction of the inhibitor with the active site thiol of the cysteine protease.

Recently we reported that compound **4** reacted rapidly with glutathione (γ-Glu-Cys-Gly tripeptide, ~2mM in plasma) to give ReO(SSS-2,2′)(SG), which could then be displaced by a free thiol (with a lower pK_a) such as thiophenol.[49] This result suggested that the rhenium complexes reported herein should undergo nucleophilic displacement with the highly nucleophilic cysteine residue in the active site of cathepsin B. Also, even if the ReO(SSS)X complexes do not remain intact in vivo and react with glutathione to give ReO(SSS)(SG), one should still observe activity against cathepsin B, albeit lower on the basis of an IC_{50} of 3.2 μM of the glutathione complex[49] (cf. compound **4** IC_{50} of 8.8 nM). The in vitro data for compounds **1**−**8** are summarized in Table 1 and reveal several interesting results.

Compounds **1** and **2** (ReO(SpyS)(SPhOMe-*p*)) exhibited moderate activity against cathepsin B with IC_{50} values of 0.9 and 6.5 μM, respectively. As expected, the monochloro complex (**1**) is more active than **2** because chloride is a better leaving group than the *p*-methoxythiophenolate. The mass spectrometry experiments (see discussion below), however, show that **2** does react significantly with cathepsin B to give the ReO(SpyS)−cathepsin B adduct, suggesting that even a compound exhibiting moderate activity will form a strong interaction with the cathepsin B active-site thiolate. Compound **3** (ReO(SSS-2,2′)-(SPhOMe-*p*)) was significantly less active (88.6 μM) than **2**, suggesting that the S atom trans to the *p*-methoxythiophenolate may stabilize the Re−S bond of the monodentate ligand. Compound **4** was extremely active against cathepsin B with an IC_{50} of 8.8 nM (~10^4 times more active than **3**) and had a potency similar to the recently reported value of the rhenium compound ReO(SSS-2,2′)(S-4py)·HCl (IC_{50} = 10 nM).[49] The green color of **4** suggests that it has a trigonal bipyramidal geometry and so will readily lose a chloride ion (upon attack from a nucleophilic cysteine thiolate in the active site of cathepsin B) to adopt the preferred square pyramidal geometry seen for all ReO(SSS)(SR) complexes reported in the literature.[50,52,53] We also investigated if our complexes would be selective for cathepsin B over cathepsin K, as was seen for several of the ReO(SSS)(SR) complexes recently reported.[49] Compound **1** shows a moderate selectivity (5-fold higher) for the inhibition of cathepsin B over cathepsin K, whereas compound **4** is very selective for cathepsin B (45-fold higher). This result supports our previous finding that complexes containing the ReO(SSS) core are the most selective metal-based inhibitors of cathepsin B reported.[49]

A comparison of the IC_{50} values for **4** (8.8 nM) and **6** (ReO-(SSS-2,2′)Br, 1.0 nM) showed that as expected the monobromo complex was more reactive than its chloro analogue; bromide is a better leaving group than chloride. This effect was also observed for complexes **5** and **8** where the bromo complex **8** (9.3 ± 0.3 μM) was more active against cathepsin B than its corresponding chloro complex **5** (11.2 ± 0.4 μM), although with the SSS-3,3′ ligand system the effect is not as pronounced (at the limits of standard error there is only up to a 20% difference in IC_{50} values). Compound **6** is the most potent metal-based inhibitor against cathepsin B reported and also shows even higher selectivity for cathepsin B over cathepsin K (260-fold

Table 1. IC_{50} (μM) of Re Compounds **1**−**8** with Cathepsins B and K

Compound	Structure	Cathepsin B IC_{50} (μM)[a]	Cathepsin K IC_{50} (μM)[a]
1		0.90 +/- 0.48	4.81 +/- 2.35
2	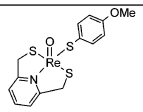	6.51 +/- 1.20	>50
3	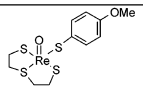	88.6 +/- 6.9	>50
4		0.0088 +/- 0.0002	0.40 +/- 0.02
5		11.2 +/- 0.4	>50
6		0.0010 +/- 0.0003	0.26 +/- 0.02
7		0.401 +/- 0.003	>50
8		9.29 +/- 0.28	>50

[a] IC_{50} values are the mean ± standard error.

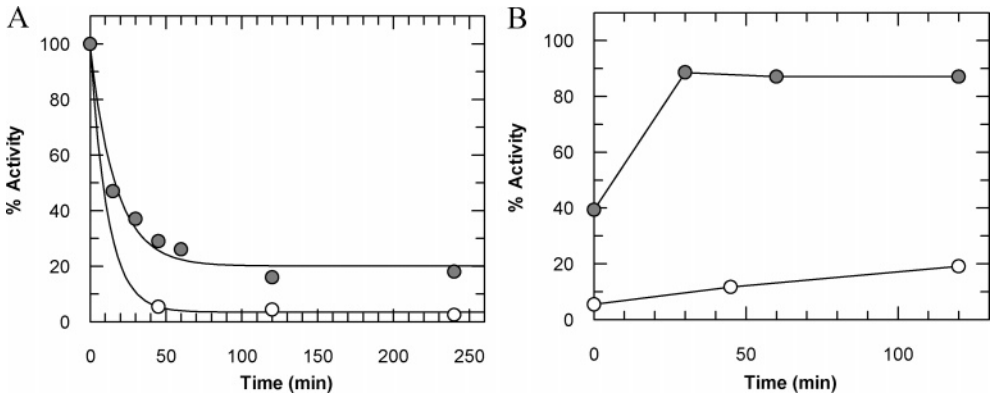

Figure 1. Time-dependent inhibition (A) and cysteine reactivation (B) of cathepsin B by 40 nM **4** (○) and 200 μM **3** (●).

higher) than compound **4**. For comparison, other metal-based inhibitors for cathepsin B include organotellurium(IV),[54] gold (I),[55] and Re(V)[49] and have potencies of 1.5, 0.6−250, and 0.01−50 μM, respectively.

We also studied the effect that modifying the linker length between the S atoms of the tridentate trithio ligand would have on the activity of the complex against cathepsins B and K. We hypothesized that increasing the linker length of the ligand SSS-2,2′ from two CH_2 groups to three sequentially to give SSS-2,3′ and SSS-3,3′ would give more stable ReO(SSS)X complexes. For a five-membered chelate the ring strain amounts to about 7 kcal mol^{-1}, while a six-membered chelate ring is virtually strain-free. The data in Table 1 show that as the total ring strain in the molecule is decreased, the activity of the complex against cathepsin B also decreases (IC_{50} values: compound **6** (5,5-bischelate), 0.001 μM; compound **7** (5,6-bischelate), 0.4 μM; compound **8** (6,6-bischelate), 9.3 μM). Presumably the Re−Br bond increases in strength as the total ring strain decreases, thus making it more difficult for the nucleophilic cysteine of cathepsin B to displace the bromide (compound **6** is $\sim 10^4$ more potent than compound **8**). There may also be a steric component to this observed effect whereby the larger six-membered chelate rings decrease the accessibility of the incoming active-site thiolates for the rhenium center. The same effect was also observed between compounds **4** and **5** where the former was $\sim 10^3$ more potent, the effect being less pronounced for the chloro derivatives over the bromo derivatives.

2.3. Mode of Inhibition. Enzyme inhibitors can be divided into two main classes, irreversible and reversible.[30,56] Irreversible-type inhibitors are compounds that bind covalently to the enzyme. Although the initial binding is reversible, the enzyme−substrate complex then undergoes a time-dependent reaction that leads to enzyme inactivation. This complexation may be either irreversible in nature, as is the case for suicide inactivators, or slowly reversible over time depending on the strength of the inhibitor−enzyme interaction. On the other hand, reversible inhibitors form a dynamic complex with the enzyme that have catalytic properties different from those of the uninhibited enzyme. Full enzymatic activity can be regained over time or in vitro by dilution, dialysis, or filtration. The classification of inhibitors is based on kinetic analysis. Simple, classical fast-binding reversible inhibitors can be defined as competitive, noncompetitive, uncompetitive, or mixed depending on how they compete with the substrate for binding to the active site. In practice it may be difficult to differentiate between reversible and irreversible inhibitors. For example, if a reversible inhibitor binds to the enzyme with such a high affinity that the enzyme−inhibitor complex dissociates very slowly, it may appear to be irreversible. They are classified as tight-binding reversible inhibitors. There are also reversible inhibitors that only inhibit enzyme activity very slowly because of conformational changes following enzyme−inhibitor complex formation and are classified as slow-binding reversible inhibitors. Generally, reversible inhibitors are preferred as potential therapeutic agents in circumstances where it is desirable for activity to be periodically restored to the enzyme so that it can carry out its normal functions when required.

Table 2. Summary of Time Dependence and Cysteine Reactivation of Cathepsin B by **4** and **2**

	% inhibition			% reactivation[a]		
	45 min	2 h	4 h	45 min	2 h	4 h
2	45	45	42	43	42	45
4	95	96	97	6	14	18

[a] % Reactivation is defined as the percent regain in activity compared to control after 45 min of incubation with compound (5 IC_{50} concentration as defined in Table 1) and then at 45 min, 2 h, or 4 h further incubation with 30 μM cysteine. Results are from duplicates of one experiment. All experiments were repeated on 2 separate days, and results did not vary by more thant ±20%.

The time dependence and cysteine reactivation properties were evaluated for **2** and **4** in order to characterize the reversibility of inhibition. After 45 min of incubation of **4** with cathepsin B (Figure 1A) there was complete inhibition and minimal recovery of activity after the addition of 30 μM cysteine (Figure 1B, Table 2), indicating that **4** is an irreversible-type inhibitor. A full analysis using the Kitz−Wilson method (equation shown below) for determination of the time dependence of inhibition by **4** with cathepsin B is shown in Figure 2.[57] Initially, quantification comes from a plot of rate versus time fitted to a single-exponential decay model to determine k_{obs} at each time point (Figure 2A). Following this, a calculation of the kinetic parameters comes from the inverse of the following expression for inactivation,

$$k_{obs(inact)} \equiv \frac{k_{inact}[I]}{K_{inact} + [I]}$$

where a plot of $1/k_{obs(inact)}$ vs $1/[I]$ is a straight line and allows one to solve for k_{inact} and K_{inact}. The inhibition by **4** is rapid and potent with a k_{inact} of 0.078 min^{-1} and a K_{inact} of 0.054 μM (Figure 2B, Table 3), where k_{inact} is the rate constant for inactivation and K_{inact} is the apparent dissociation constant of all bound enzyme species, as shown below:

$$E + I \overset{K_{inact}}{\longleftrightarrow} E{\cdot}I \xrightarrow{k_{inact}} E{-}I$$

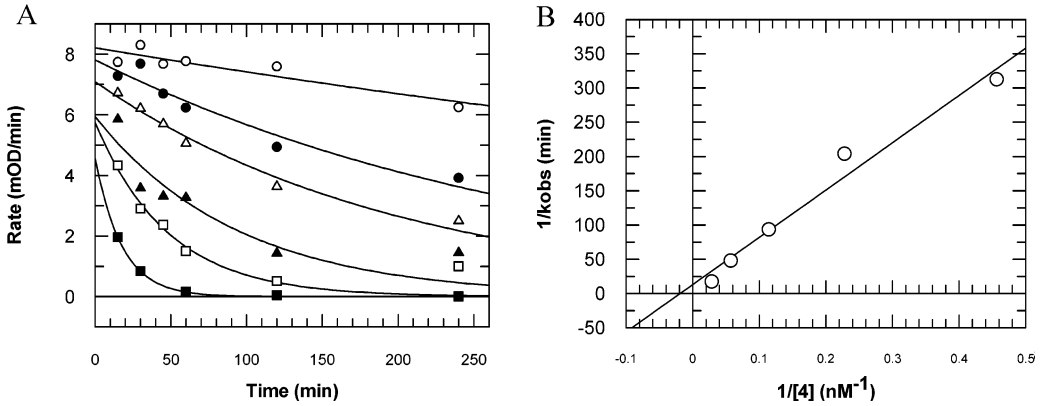

Figure 2. (A) Time-dependent inhibition of cathepsin B in the presence of **4** (no inhibitor (○), 2.2 nM **4** (●), 4.38 nM **4** (△), 8.75 nM **4** (▲), 17.5 nM **4** (□), 35 nM **4** (■). (B) $K_{inact}-k_{inact}$ plot for the determination of kinetic parameters.

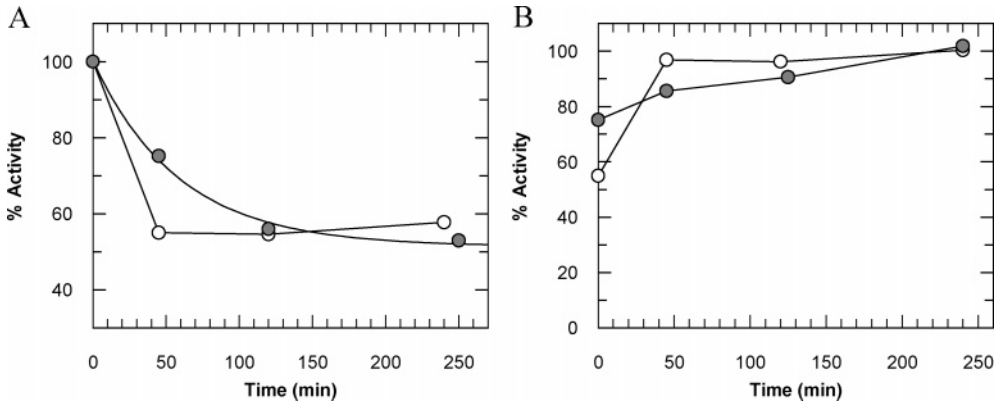

Figure 3. Time-dependent inhibition (A) and cysteine reactivation (B) of cathepsin B by 5.2 μM **2** (○) and 0.5 μM **1** (●).

Table 3. Summary of the Kinetic Parameters and Mode of Inhibition Determined for the Inhibition of Cathepsin B with **2** and **4**

	mode of inhibition	parameter	IC_{50} (μM)
2	competitive	$K_i = 0.086 \pm 0.017$ μM	6.51
4	time-dependent	$k_{inact} \approx 0.078$ min^{-1}	0.0088
		$K_{inact} \approx 0.054$ μM	

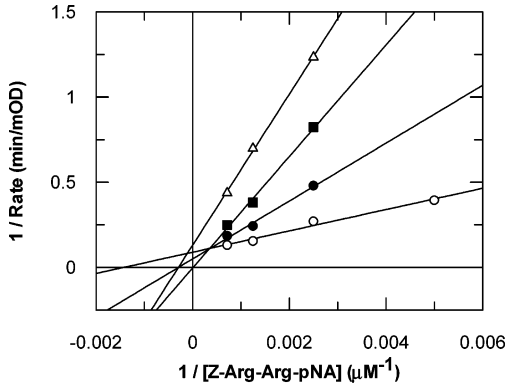

Figure 4. Lineweaver−Burke determination for the K_i of **2** with cathepsin B, with the following concentrations for **2**: 0 μM (○), 0.1 μM (●), 0.4 μM (■), 0.8 μM (▲).

When the inhibition of cathepsin B by **2** was examined over time, the enzyme activity was only inhibited by 50%, even after 4 h of incubation with **2** (Figure 3A). This is the typical inhibition pattern of a slow-binding reversible inhibitor, where it takes a finite length of time to establish maximal inhibition (in this case 45 min), after which time no further inhibition is obtained. Furthermore, the addition of 30 μM cysteine results in full recovery of activity within 45 min (Figure 3B). A similar pattern of inhibition and reactivation was observed for **1**. The choice of leaving group (chloro versus SphOMe-*p*) did not affect the rate of inhibition or its reversibility. These data are summarized in Table 2.

As discussed above in the initial study with compound **2**, no exponential decay of enzyme activity was observed that would have indicated a time-dependent inhibitor. Instead, a certain amount of inhibition is achieved and remains constant over time. A similar pattern of inhibition was observed when the compound was tested over a range of concentrations. When both the concentrations of compound **2** and substrate are varied and plotted according to the Lineweaver−Burke analysis, the data are consistent with a model approximating competitive inhibition with a K_i of 0.086 ± 0.017 μM (Figure 4). Analysis by an Eadie−Hofstee plot led to a similar conclusion (plot not shown). The enzyme kinetics equation in the presence of a competitive inhibitor is shown below.

$$v = \frac{V_{max}[S]}{K_m\left(1 + \frac{[I]}{K_i}\right) + [S]}$$

2.4. Active-Site Titration and Protection from Inactivation. A quantification of the number of active sites actually present in an enzyme solution is possible with a potent irreversible inhibitor of cathepsin B, L-*trans*-epoxysuccinylleucylamido(4-guanidino)butane (E-64), isolated from cultures of *Aspergillus japonicus*.[32] According to the method of Barrett et al., it reacts stoichiometrically in a 1:1 manner with cathepsin B, and by extrapolation on the *x*-axis to zero enzyme activity in a rate of enzyme activity versus concentration of inactivation plot, the active site concentration of enzyme can be obtained (Figure 5). Typically with cathepsin B, 30−50% of the active sites as

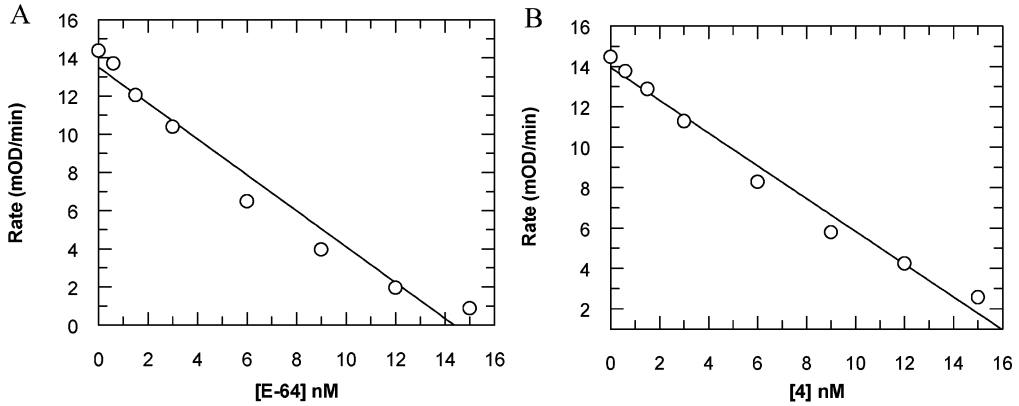

Figure 5. Titration of the active sites of cathepsin B using (A) E-64 and (B) **4**.

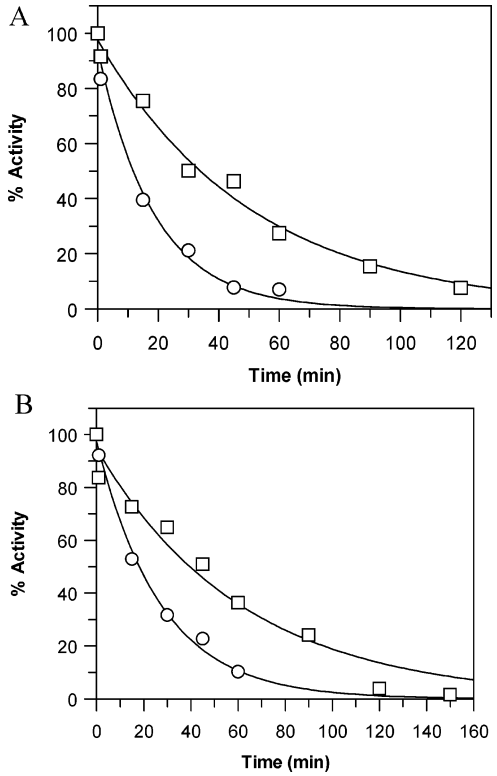

Figure 6. (A) Inactivation of cathepsin B by 10 nM **4** (○) and protection from inactivation by 10 nM **4** in the presence of 0.5 μM chymostatin (□). (B) Inactivation of cathepsin B by 10 nM E-64 (○) and protection from inactivation by 10 nM E-64 in the presence of 0.5 μM chymostatin (□).

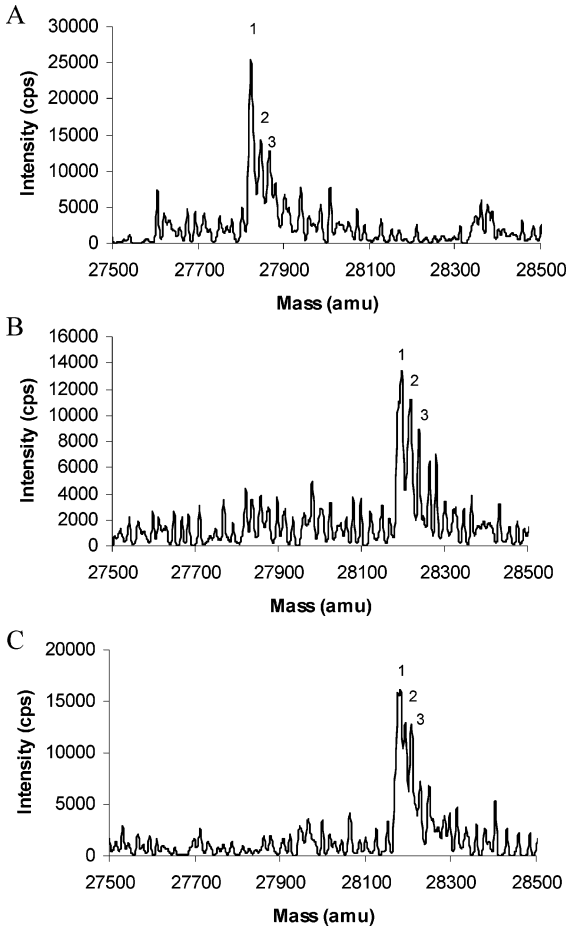

Figure 7. (A) Mass spectrum of cathepsin B (peak 1 = 27 823 Da, peak 2 = 27 847 Da, peak 3 = 27 868 Da); (B) mass spectrum of cathepsin B with **4** (peak 1 = 28 199 Da, peak 2 = 28 220 Da, peak 3 = 28 239 Da); (C) mass spectrum of cathepsin B with **2** (peak 1 = 28 176 Da, peak 2 = 28 192 Da, peak 3 = 28 208 Da).

calculated by protein molecular weight are inactivated by E-64 titration, but the nature of the inactivatable component of the enzyme preparation is unknown.[32] In this study, the molarity of the activated enzyme solution using E-64 titration was found to be 14.4 nM (Figure 5A) and on the basis of the starting concentration of 18 nM cathepsin B, at least 80% of the enzyme is activated. As described in the Experimental Section, the activated enzyme is that enzyme with the active site cysteine in the reduced form and available for catalysis. When the same method was used, the molarity of the activated enzyme solution using **4** was found to be 17 nM (Figure 5B), and because it is known that E-64 reacts with cathepsin B in a 1:1 ratio, it can be assumed that 1 equiv of **4** must also react with the enzyme, indicating that both inhibitors are active-site-directed.

Further proof for the active-site-directed nature of **4** was afforded from protection from inactivation experiments using chymostatin, a known reversible inhibitor of cathepsin B.[29] The assumption is that if the inactivation is directed to the active site where chemical catalysis occurs, a known competitive inhibitor will act in the same subsite of the active site and thereby block the inactivator from reaching its point of action. This will result in a slower rate of inactivation ($k_{obs(inact)}^{prot}$). At the concentration of chymostatin employed (IC_{50}), approximately 38% protection from inactivation by **4** was afforded (Figure 6A). By use of a combination of the equation for competing substrates with the Kitz−Wilson scheme for enzyme inactivation, the resulting rate equation can be used to compare the calculated rate of inactivation in the presence of a competitive inhibitor with that obtained experimentally as shown below

where P is the competitive inhibitor with a dissociation constant of K_d.[57−59]

$$\frac{k_{obs(inact)}^{prot}}{k_{obs(inact)}} = \frac{k_{inact} + [I]}{K_{inact}(1 + [P]/K_d) + [I]}$$

The k_{obs} determined in the presence of 0.5 μM chymostatin ($k_{obs(inact)}^{prot}$) = 0.010 min^{-1}) agrees well with the expected calculated rate of inactivation using the previously determined K_{inact} and k_{inact} ($k_{obs(inact)}^{prot}$ = 0.014 min^{-1}). This provides additional strong evidence that **4** reacts at the active site. A comparative control experiment was performed with E-64, a known irreversible active-site-directed inhibitor of cathepsin B. As shown in Figure 6B, in this instance, chymostatin provided 37% protection of inactivation by E-64, providing support to the previously reported observations in the literature that E-64 is an active-site-directed irreversible inactivator.[60]

2.5. Mass Spectral Studies. As shown in Figure 7A, human liver cathepsin B was found to have an average molecular weight of 27823 ± 5 Da. As is evident by the higher molecular weight species in the spectrum, human liver cathepsin B is glycosylated. Upon incubation of cathepsin B with an excess of **4**, an increase in molecular weight equivalent to one **4** moiety minus the chloride group on the intact protein {(27 823 + 354 Da) ± 5 Da} was observed by ES-MS (Figure 7B). Similar ES-MS analysis of cathepsin B incubated with **2** revealed a mass increase of {27 823 + 372 Da) ± 5 Da} consistent with the formation of a cathepsin B−compound **2** complex with the loss of the methoxythiol phenol leaving group (Figure 7C). Both experiments provide evidence for the existence of 1 equiv of inhibitor binding to cathepsin B, likely through the formation of a dithiol bond between the sulfur of the inhibitor and the free cysteine of the active site. Regardless of whether the inhibition is reversible or irreversible in nature, the turnover rate of the enzyme−inhibitor complex is low enough that accumulation of an inhibitor intermediate could be observed by ES-MS following 1 h of incubation of enzyme and inhibitor. This provides conclusive evidence of the formation of a rhenium−cathepsin B intermediate.

3. Conclusions

In this paper we reported the synthesis and characterization of two new tridentate ligands (3,3′-thiodipropanethiol (HSSSH-3,3′) and thio-2-ethanethiol-3′-propanethiol (HSSSH-2,3′)) and their corresponding oxorhenium(V) complexes ReO(SSS-3,3′)X (X = Cl, Br) and ReO(SSS-2,3′)Br. We also discovered that the ReO(SpyS)Cl complex, which several groups have attempted to synthesize in the past, could be isolated by treating [$BzEt_3N$][$ReOCl_4$] with a mixture of HSpySH and 4,6-dihydroxy-2-mercaptopyridine and allowing the slow displacement of the monodentate thiol by chloride in situ.

The evaluation of the rhenium complexes as potential inhibitors against cathepsins B and K was performed in vitro. The ReO(SXS)(SPhOMe-*p*) (X = S (**3**), py (**2**)) complexes exhibited a low to moderate inhibitory effect on cathepsin B ((IC_{50} = 88 and 6.5 μM, respectively) and no inhibition of cathepsin K. The chloro analogue of **2**, compound **1**, showed increased potency over **2** against both cathepsin B ((IC_{50} = 0.9 μM) and cathepsin K ((IC_{50} = 4.8 μM). The complexes ReO(SSS)X (X = Cl, Br) were quite potent inhibitors against cathepsin B, and it was discovered that the potency of the compound was directly related to the size of the chelate rings in the tridentate ligand (IC_{50}: compound **6** (5,5-bischelate), 0.001 μM; compound **7** (5,6-bischelate), 0.4 μM; compound **8** (6,6-bischelate), 9.3 μM); the larger is the chelate, the less potent is the compound. The most active compounds against cathepsin B were **4** and **6** (IC_{50} = 0.009 and 0.001 μM, respectively). It was also observed that all of the complexes reported here showed a higher selectivity for cathepsin B over cathepsin K; in particular, compounds **4** (45-fold) and **6** (260-fold) exhibited excellent selectivity. To our knowledge, compound **6** is the most potent metal-based inhibitor against cathepsin B ((IC_{50} = 0.001 μM) and cathepsin K ((IC_{50} = 0.26 μM) reported to date.

The mechanism of inhibition was also studied for two of the compounds (**2** and **4**). With standard determinations of kinetic parameters, active-site titration, and active-site protection with chymostatin, it was concluded that both **2** (ReO(SpyS)(S-PhOMe-*p*) and **4** ReO(SSS-2,2′)Cl were selective active-site-directed inhibitors of cathepsin B. Mechanistically, however, they were different because compound **2** was a tight-binding reversible inhibitor while compound **4** was a time-dependent inhibitor, only slowly reversed in the presence of an exogenous thiol-like cysteine. However, mass spectrometry studies showed accumulation of a cathepsin B−rhenium complex intermediate for both compounds, providing further conclusive evidence of the active-site-directed nature of the inhibition. These results indicate that the potency and reversibility of the oxorhenium complexes toward cathepsin B may make them a useful therapeutic treatment against cancer.

4. Experimental Section

4.1. Materials. Most of the reagents and solvents were purchased at the highest commercial quality and used without further purification. The ligand HSSSH-2,2′ was purchased from Aldrich Chemical Co., and HSpySH was synthesized according to a literature procedure;[61] the ligands HSSSH-2,3′ and HSSSH-3,3′ were made as described in the synthesis section below. The precursor complexes [$BzEt_3N$][$ReOCl_4$][51] and [Bu_4N][$ReOBr_4$][62] were synthesized according to a literature procedure. Complexes **2**,[63] **3**,[64] **4**,[51] and **6**[65] were synthesized according to procedures previously reported in the literature.

^{1}H NMR spectra were recorded on a Bruker Avance 300 spectrometer with ^{1}H shifts referenced to the residual proton shift of the internal deuterated solvent. IR spectra (as KBr pellets) were recorded on a Mattson Galaxy series 5000 FTIR spectrophotometer (only the Re═O band is reported for each complex). Electrospray mass spectra were recorded on a Bruker-HP Esquire-LC ion trap mass spectrometer. Elemental analyses were performed by Atlantic Microlab, Inc. (Norcross, GA).

4.2. Synthesis. 4.2.1. ReO(SpyS)Cl (1). [$BzEt_3N$][$ReOCl_4$] (0.374 g, 0.70 mmol) in methanol (15 mL) was added to a mixture of HSpySH (0.119 g, 0.70 mmol) and 4,6-dihydroxy-2-mercaptopyridine (0.066 g, 0.70 mmol) in chloroform (15 mL). The resulting red-brown solution was stirred at room temperature for 18 h to yield a clear, brown solution with a dark-green precipitate. The green solid was isolated via suction filtration, washed with acetonitrile (2 × 3 mL) and diethyl ether (3 × 5 mL), and dried in vacuo (0.089 g, 31%). ^{1}H NMR (CD_2Cl_2) δ 5.04 (d, 2H, J = 18.3 Hz), 5.64 (d, 2H, J = 18.3 Hz), 7.97 (d, 2H, J = 7.5 Hz), 8.15 (t, 1H, J = 7.5 Hz). ES-MS m/z 430 [M + Na]$^+$. IR (KBr) ν (cm^{-1}) 985 (Re═O). Anal. ($C_7H_7NOS_2ClRe\cdot 0.1C_2H_3N$) C, H, N, S, Cl.

4.2.2. ReO(SSS-3,3′)Cl (5). 4.2.2.1. 3,3′-Thiodipropanethiol (HSSSH-3,3′). 3,3′-Thiodipropanol (1.97 g, 13.1 mmol) was dissolved in methylene chloride (100 mL) to give a clear, colorless solution. Triethylamine (3.84 mL, 27.6 mmol) was added, and the mixture was cooled to 0 °C. Methanesulfonyl chloride (2.03 mL, 26.2 mmol) was added dropwise via syringe, resulting in the formation of a white slurry. The mixture was stirred for 3 h at room temperature. The mixture was washed with saturated NH_4Cl, dried over Na_2SO_4, and concentrated under reduced pressure to yield the dimesylate as a white solid (4.01 g, 100%). ^{1}H NMR ($CDCl_3$) δ 2.01 (p, 4H, J = 6.0 Hz), 2.63 (t, 4H, J = 7.2 Hz), 3.01

(s, 6H), 4.32 (t, 4H, $J = 6.0$ Hz). ^{13}C NMR ($CDCl_3$) δ 28.15, 29.24, 37.75, 68.57.

The dimesylate (4.01 g, 13.1 mmol) was dissolved in anhydrous tetrahydrofuran (100 mL) to give a pale-pink solution. Triethylamine (3.73 mL, 26.8 mmol) and thiolacetic acid (1.89 mL, 26.4 mmol) were added, and the now yellow mixture was refluxed for 6 h (the reaction was monitored by TLC). The mixture was then concentrated under reduced pressure and purified by column chromatography on silica gel (CH_2Cl_2). The major band yielded the dithioacetate as a pale-orange oil (1.71 g, 49%) after drying in vacuo for 24 h. ^{1}H NMR ($CDCl_3$) δ 1.83 (p, 4H, $J = 6.0$ Hz), 2.31 (s, 6H), 2.53 (t, 4H, $J = 6.0$ Hz), 2.94 (t, 2H, $J = 6.0$ Hz). ^{13}C NMR ($CDCl_3$) δ 28.28, 29.61, 30.94, 195.65.

The dithioacetate (1.71 g, 6.43 mmol) was dissolved in methanol (40 mL) to give a yellow solution. An amount of 8 mL of 6 N HCl was added, and the mixture was refluxed for 16 h when TLC no longer revealed the presence of the dithioacetate. The solvent was removed under reduced pressure to yield pure dithiol as an orange oil (1.00 g, 86%). ^{1}H NMR ($CDCl_3$) δ 1.35 (t, 2H, $J = 7.5$ Hz), 1.85 (p, 4H, $J = 6.0$ Hz), 2.60 (m, 8H). ^{13}C NMR ($CDCl_3$) δ 23.82, 30.66, 33.66.

4.2.2.2. Preparation of ReO(SSS-3,3′)Cl. [$BzEt_3N$][$ReOCl_4$] (0.656 g, 1.22 mmol) was dissolved in anhydrous methanol (15 mL) under 1 atm of argon at room temperature to give a green solution. HSSSH-3,3′ (0.188 g, 1.29 mmol) dissolved in 3 mL of chloroform was added dropwise via syringe, resulting in an olive slurry. The reaction mixture was stirred at room temperature for 3 h, and the final slurry was filtered. The isolated olive solid was washed with methanol (3×5 mL) and chilled methylene chloride (2×5 mL) to yield a lime-green solid, which was dried in vacuo (0.045 g, 14%). ^{1}H NMR (CD_2Cl_2) δ 2.37 (m, 2H), 3.00 (m, 6H), 3.79 (m, 2H), 4.20 (m, 2H). IR (KBr) ν (cm^{-1}) 972 (Re═O). Anal. ($C_6H_{12}OS_3ClRe$) C, H, S, Cl.

4.2.3 ReO(SSS-2,3′)Br (7). 4.2.3.1. Thio-2-ethanethiol-3′-propanethiol (HSSSH-2,3′). 3-Mercaptopropanol (2 mL, 2.13 g, 23.1 mmol) was dissolved in anhydrous tetrahydrofuran (100 mL). Triethylamine (3.22 mL, 23.1 mmol) was added, and the reaction solution was cooled to 0 °C. Ethylene oxide was bubbled through the solution for 30 min, and then the vessel was sealed and allowed to warm to room temperature. The mixture was stirred for 16 h when the ^{1}H NMR spectrum of the crude mixture indicated all of the 3-mercaptopropanol had reacted, presumably giving the desired diol.

The crude diol was concentrated under reduced pressure and then dissolved in methylene chloride (50 mL) to give a clear, colorless solution. Triethylamine (6.45 mL, 46.3 mmol) was added, and the mixture was cooled to 0 °C. Methanesulfonyl chloride (3.57 mL, 46.2 mmol) was added dropwise via syringe, resulting in the formation of a white slurry. The mixture was stirred for 14 h at room temperature. The mixture was washed with saturated NH_4-Cl, dried over Na_2SO_4, and concentrated under reduced pressure to give a colorless oil. The crude oil was purified using column chromatography on silica gel (CH_2Cl_2) to yield the mixed-mesyl/chloro compound $MsOCH_2CH_2CH_2SCH_2CH_2Cl$ as a pure colorless oil (3.52 g, 65%). ^{1}H NMR ($CDCl_3$) δ 1.98 (p, 2H, $J = 6.8$ Hz), 2.64 (t, 2H, $J = 7.1$ Hz), 2.83 (t, 2H, $J = 6.9$ Hz), 2.96 (s, 3H), 3.58 (t, 2H, $J = 7.0$ Hz), 4.27 (t, 2H, $J = 6.8$ Hz). ^{13}C NMR ($CDCl_3$) δ 28.41, 29.40, 34.54, 37.68, 43.51, 68.55.

The mixed-mesyl/chloro compound (3.52 g, 15.1 mmol) was dissolved in anhydrous tetrahydrofuran (80 mL) to give a colorless solution. Triethylamine (4.21 mL, 30.2 mmol) and thiolacetic acid (2.16 mL, 30.2 mmol) were added, and the now yellow mixture was refluxed for 18 h (the reaction was monitored by TLC). The mixture was then concentrated under reduced pressure and purified by column chromatography on silica gel (CH_2Cl_2). The major band yielded the dithioacetate as a pale-orange oil (1.17 g, 31%) after drying in vacuo for 24 h. ^{1}H NMR ($CDCl_3$) δ 1.88 (p, 2H, $J = 9.0$ Hz), 2.34 (s, 3H), 2.35 (s, 3H), 2.67 (m, 4H), 2.98 (t, 2H, $J = 9.0$ Hz), 3.07 (t, 2H, $J = 6.0$ Hz). ^{13}C NMR ($CDCl_3$) δ 28.32, 29.59, 29.68, 31.06, 32.03, 195.62, 195.98.

The dithioacetate (1.17 g, 4.66 mmol) was dissolved in methanol (60 mL) to give a yellow solution. An amount of 15 mL of 6 N HCl was added, and the mixture was refluxed for 18 h when TLC no longer revealed the presence of the dithioacetate. The solvent was removed under reduced pressure to yield pure dithiol as an orange oil (0.73 g, 93%). ^{1}H NMR ($CDCl_3$) δ 1.34 (t, 1H, $J = 8.1$ Hz), 1.72 (t, 1H, $J = 7.2$ Hz), 1.83 (p, 2H, $J = 6.9$ Hz), 2.60 (m, 4H), 2.69 (m, 4H). ^{13}C NMR ($CDCl_3$) δ 23.78, 25.14, 30.59, 33.70, 36.47.

4.2.3.2. Preparation of ReO(SSS-2,3′)Br. [Bu_4N][$ReOBr_4$] (0.307 g, 0.40 mmol) was dissolved in anhydrous methylene chloride (10 mL) under 1 atm of argon at room temperature to give a pink-purple solution. HSSSH-2,3′ (0.071 g, 0.42 mmol) dissolved in 3 mL of methylene chloride was added dropwise via syringe, resulting in a dark-green solution. The reaction mixture was stirred at room temperature for 1 h. Addition of methanol (20 mL) yielded a dark-green precipitate, which was isolated via suction filtration and washed with methanol (3×5 mL) and chilled methylene chloride (2×2 mL) to yield a lime-green solid, which was dried in vacuo (0.026 g, 14%). ^{1}H NMR (CD_3CN) δ 2.63 (m, 2H), 2.91 (td, 1H, $J = 4.5$, 10.8 Hz), 3.05 (m, 2H), 3.34 (m, 2H), 3.53 (m, 2H), 3.91 (m, 1H). IR (KBr) ν (cm^{-1}) 968 (Re═O). Anal. ($C_5H_{10}OS_3BrRe$) C, H, S, Br.

4.2.4. ReO(SSS-3,3′)Br (8). [Bu_4N][$ReOBr_4$] (0.302 g, 0.39 mmol) was dissolved in anhydrous methylene chloride (10 mL) under 1 atm of argon at room temperature to give a pink-purple solution. HSSSH-3,3′ (0.188 g, 1.29 mmol) dissolved in 3 mL of methylene chloride was added dropwise via syringe, resulting in a dark-green solution. The reaction mixture was stirred at room temperature for 1 h. Addition of methanol (20 mL) yielded a dark-green precipitate, which was isolated via suction filtration and washed with methanol (3×5 mL) and chilled methylene chloride (2×5 mL) to yield a lime-green solid, which was dried in vacuo (0.037 g, 20%). ^{1}H NMR (CD_2Cl_2) δ 2.38 (m, 2H), 2.98 (m, 6H), 3.76 (d, 2H, $J = 7.5$ Hz), 4.20 (m, 2H). IR (KBr) ν (cm^{-1}) 974 (Re═O). Anal. ($C_6H_{12}OS_3BrRe$) C, H, S, Br.

4.3. Methods. 4.3.1. Enzymology. All buffer chemicals were analytical or reagent grade and were purchased from Sigma or Calbiochem. Human liver cathepsin B was obtained from Athens Research and Technology Company (Athens, GA), and human cathepsin K was cloned, expressed, and purified in-house using similar procedures previously reported for cathepsins B and L.[66] The substrate Z-Arg-Arg-pNa, as well as the inhibitor E-64, and BRIJ (a nonionic detergent composed of polyoxyethylene lauryl ether and polyoxyethylene glycol dodecyl ether) were from Calbiochem. The substrate Z-Val-Arg-AMC was from Novochem. All data were analyzed using the software package Grafit, version 4.09.[67] All kinetic experiments were done in triplicate and repeated on separate days for consistency. Replicate experiments were compared by calculating mean values with associated standard errors and using the *t*-test where appropriate. A representation of one single experiment is provided in the text for discussion purposes.

4.3.2. IC_{50} Determinations. IC_{50} determinations were performed in duplicate with constant enzyme and substrate concentrations while varying the inhibitor concentration. Inhibitor concentrations ranged from 7 nM to 25 μM. Serial dilution of inhibitor was done on the MultiPROBE robot liquid handling workstation (Packard) in 96-well plates (Falcon). Enzyme and inhibitor were co-incubated at 30°C for 45 min prior to the addition of substrate. Activity was measured over 3 min at 410 nm for pNA or at 355 nm excitation and 460 nm emission for 7-AMC fluorescent detection. Colormetric readings were made on a SpectraMAX, and fluorescent readings were made on a FMAX, both from Molecular Devices.

The colorimetric cathepsin B assay was performed in 100 mM sodium phosphate, 1 mM EDTA, 0.025% BRIJ, 1.25 μM DTT, pH 6.0, using 10 nM enzyme and 1 mM Z-Arg-Arg-pNA. In order for the enzyme to be catalytically functional, the active site cysteine needs to be in a reduced form. Because the cysteine is readily oxidized through contact with air, prior to use it needs to be pretreated with a reducing agent like DTT to ensure that the majority

of the enzyme is in a catalytically active form. Therefore, prior to dilution, 0.2 mg/mL cathepsin B was activated in the presence of 0.4 mM dithiothreitol for 1 h at 30 °C. The cathepsin K assay was performed in 100 mM sodium acetate, 5 mM EDTA, 0.003% BRIJ, 10 μM DTT, pH 5.5, with 10 nM enzyme and 10 μM Z-Val-Arg-AMC. Similarily, prior to use, cathepsin K was activated at 30 °C in buffer containing 0.003% BRIJ and 10 μM DTT for a minimum of 20 min.

4.3.3. Mode of Inhibition Analysis. The reversible inhibition constant, K_i, was determined for **2** with cathepsin B. Compound **2** was tested at concentrations ranging from 0.1 to 0.8 μM using a 45 min enzyme−inhibitor preincubation. The substrate Z-Arg-Arg-pNA was added at concentrations ranging from 200 μM to 1.3 mM. The inhibition for **4** was evaluated using a single enzyme and substrate concentration, with analysis over a 4 h time period. Concentrations of **4** ranged from 2.2 to 35 nM.

Initial time dependence was evaluated using an inhibitor concentration of approximately 5 IC_{50}. Time dependence of inhibition was assessed, after the reaction was initiated ($t = 0$ min), at 45 min, 2 h, and 4 h of enzyme−inhibitor incubation at 30 °C. Substrate (1 mM Z-Arg-Arg-pNA) was added following the specified incubation period, and activity was read. Buffer and enzyme concentrations were as described above. The full time-dependent inhibition analysis for **4** against cathepsin B was evaluated over a concentration range of **4** from 2.2 to 35 nM.

4.3.4. Cysteine Reactivation. Cysteine reactivation was evaluated using an inhibitor concentration of approximately the IC_{50} up to 5 IC_{50}, depending on the potency of the inhibitor and an upper limit constraint to keep the solvent in the reaction mix at a minimum. The enzyme−inhibitor incubation times for the cysteine reactivation assay were 45 min, 2 h, and 4 h after an initial 45 min incubation with compound. After the initial 45 min incubation, 30 μM cysteine was added, and incubation was continued for the required time at 30 °C. Following incubation, substrate was added and activity was read. Buffer, enzyme, and substrate concentrations were as described above.

4.3.5. Active-Site Titration and Protection from Inactivation. For the active-site titration experiments, E-64 (L-*trans*-epoxysuccinylleucylamido(4-guanidino)butane) was dissolved in 1 mM in dimethyl sulfoxide, then diluted in 100 mM sodium phosphate, 1 mM EDTA, 0.025% BRIJ, and 1.25 μM DTT. Enzyme and substrate were used at the following concentrations: cathepsin B, 18 nM; Z-Arg-Arg-pNA, 1 mM. E-64 or **4** was used at concentrations ranging from 0.1 to 5.0 nM. A control in the absence of E-64 or **4** was included. Samples were performed in duplicate at a final volume of 100 μL. Enzyme, buffer, and E-64 or compound **4** were incubated at 30 °C for 1.5 h prior to substrate addition and plate reading. Activity, in RFU/min, was plotted as a function of concentrations of E-64 or compound **4**. The linear portion of the curve was extrapolated to obtain the value at the abscissa, which defines the active-site concentration. The percentage of active protein was calculated on the basis of the ratio of the active site and total protein concentrations.

For the protection from inactivation experiments, E-64 was dissolved in 1 mM in dimethyl sulfoxide, then diluted in 100 mM sodium phosphate, 1 mM EDTA, 0.025% BRIJ, 1.25 μM DTT, pH 6.0, to a final assay concentration of 10 nM. Cathepsin B and Z-Arg-Arg-pNA were used at concentrations of 18 nM and 1 mM, respectively. Chymostatin and **4** were at concentrations of 0.5 μM and 10 nM, respectively. Cathepsin B was incubated with chymostatin and either E-64 or **4**, and substrate was added and activity read at time points up to 2 h. Samples were performed in duplicate at a final volume of 100 μL.

4.3.6. Mass Spectrometry. The analyses of protein samples were carried out using a Sciex API-300 mass spectrometer interfaced with a Michrom UMA HPLC system (Michrom Bioresources, Inc., Pleasanton, CA). Cathepsin B was activated in the presence of DTT prior to use as described above. Cathepsin B (10−20 μg in 20 mM sodium acetate buffer, pH 5.0, 1 mM EDTA) was first incubated for 1 h at 30 °C in the presence of excess **2** (227 μM) or **4** (454 μM). Immediately after the incubation period, the residual activity of the mixtures was analyzed as described above using the standard assay conditions and then cathepsin B alone, or the cathepsin B−inhibitor mixture was introduced into the mass spectrometer through a microbore PLRP column (1 mm × 50 mm) and eluted with a gradient of 10−100% solvent B at a flow rate of 50 μL/min over 7 min (solvent A is 0.06% trifluoroacetic acid and 2% acetonitrile in water; solvent B is 0.05% trifluoroacetic acid and 90% acetonitrile in water). The mass spectra were obtained over the range 400−2000 Da with a step size of 0.5 Da and a dwell time of 1 ms.

Supporting Information Available: Elemental analysis results for compounds **1**, **5**, **7**, and **8**. This material is available free of charge via the Internet at http://pubs.acs.org.

References

(1) Bromme, D.; Okamoto, K. Human Cathepsin O2, a Novel Cysteine Protease Highly Expressed in Osteoclastomas and Ovary Molecular Cloning, Sequencing and Tissue Distribution. *Biol. Chem. Hoppe−Seyler* **1995**, *376*, 379−384.

(2) Duffy, M. J. Proteases as Prognostic Markers in Cancer. *Clin. Cancer Res.* **1996**, *2*, 613−618.

(3) Szpaderska, A. M.; Frankfater, A. An Intracellular Form of Cathepsin B Contributes to Invasiveness in Cancer. *Cancer Res.* **2001**, *61*, 3493−3500.

(4) Van Noorden, C. J.; Jonges, T. G.; Meade-Tollin, L. C.; Smith, R. E.; Koehler, A. In Vivo Inhibition of Cysteine Proteinases Delays the Onset of Growth of Human Pancreatic Cancer Explants. *Br. J. Cancer* **2000**, *82*, 931−936.

(5) Kos, J.; Lah, T. Cysteine Proteinases and Their Endogenous Inhibitors: Target Proteins for Prognosis, Diagnosis and Therapy in Cancer. *Oncol. Rep.* **1998**, *5*, 1349−1361.

(6) Mackey, Z. B.; O'Brien, T. C.; Greenbaum, D. C.; Blank, R. B.; McKerrow, J. H. A Cathepsin B-Like Protease Is Required for Host Protein Degradation in *Trypanosoma brucei*. *J. Biol. Chem.* **2004**, *279*, 48426−48433.

(7) Katunuma, N.; Kominami, E. Distributions and Localizations of Lysosomal Cysteine Proteinases and Cystains. *Rev. Physiol. Biochem. Pharmacol.* **1987**, *108*, 1−20.

(8) Werb, Z. Proteinases and Matrix Degradation. In *Textbook of Rheumatology*; Kelley, W. N., et al., Eds.; W. B. Saunders Co.: Philadelphia, PA, 1989; pp 300−321.

(9) Sloane, B. F.; Moin, K.; Krepela, E.; Rhozhin, J. Cathepsin B and Its Endogenous Inhibitors: The Role in Tumor Malignancy. *Cancer Metastasis Rev.* **1990**, *9*, 333−352.

(10) Troy, A. M.; Sheahan, K.; Mulcahy, H. E.; Duffy, M. J.; Hyland, J. M.; O'Donoghue, D. P. Expression of Cathepsin B and L Antigen and Activity Is Associated with Early Colorectal Cancer Progression. *Eur. J. Cancer* **2004**, *40*, 1610−1616.

(11) Sinha, A. A.; Quast, B. J.; Wilson, M. J.; Fernandes, E. T.; Reddy, P. K.; Ewing, S. L.; Sloane, B. F.; Gleason, D. F. Ratio of Cathepsin B to Stefin A Identifies Heterogeneity within Gleason Histologic Scores for Human Prostate Cancer. *Prostate* **2001**, *48*, 274−284.

(12) Ebert, M. P.; Kruger, S.; Fogeron, M. L.; Lamer, S.; Chen, J.; Pross, M.; Schulz, H. U.; Lage, H.; Heim, S.; Roessner, A.; Malfertheiner, P.; Rocken, C. Overexpression of Cathepsin B in Gastric Cancer Identified by Proteome Analysis. *Proteomics* **2005**, *5*, 1694−1704.

(13) Niedergethmann, M.; Wostbrock, B.; Sturm, J. W.; Willeke, F.; Post, S.; Hildenbrand, R. Prognostic Impact of Cysteine Proteases Cathepsin B and Cathepsin L in Pancreatic Adenocarcinoma. *Pancreas* **2004**, *29*, 204−211.

(14) Kayser, K.; Richter, N.; Hufnagl, P.; Kayser, G.; Kos, J.; Werle, B. Expression, Proliferation Activity and Clinical Significance of Cathepsin B and Cathepsin L in Operated Lung Cancer. *Anticancer Res.* **2003**, *23*, 2767−2772.

(15) Saleh, Y.; Siewinski, M.; Sebzda, T.; Jelen, M.; Ziolkowski, P.; Gutowicz, J.; Grybos, M.; Pawelec, M. Inhibition of Cathepsin B Activity in Human Breast Cancer Tissue by Cysteine Peptidase Inhibitor Isolated from Human Placenta: Immunohistochemical and Biochemical Studies. *Folia Histochem. Cytobiol.* **2003**, *41*, 161−167.

(16) Hook, V.; Toneff, T.; Bogyo, M.; Greenbaum, D.; Medzihradszky, K. F.; Neveu, J.; Lane, W.; Hook, G.; Reisine, T. Inhibition of Cathepsin B Reduces Beta-Amyloid Production in Regulated Secretory Vesicles of Neuronal Chromaffin Cells: Evidence for Cathepsin B as a Candidate Beta-Secretase of Alzheimer's Disease. *Biol. Chem.* **2005**, *386*, 931−940.

(17) Fernandez, P.; Farre, X.; Nadal, A.; Fernandez, E.; Peiro, N.; Sloane, B. F.; Sih, G.; Chapman, H. A.; Campo, E.; Cardesa, A. Expression of Cathepsins B and S in the Progression of Prostate Carcinoma. *Int. J. Cancer* **2001**, *95*, 51−55.

(18) Ishibashi, O.; Mori, Y.; Kurokawa, T.; Kumegawa, M. Breast Cancer Cells Express Cathepsins B and L but Not Cathepsins K or H. *Cancer Biochem. Biophys.* **1999**, *17*, 69−78.
(19) Osmak, M.; Svetic, B.; Gabrijelcic-Geiger, D.; Skrk, J. Drug-Resistant Human Laryngeal Carcinoma Cells Have Increased Levels of Cathepsin B. *Anticancer Res.* **2001**, *21*, 481−484.
(20) Satoh, Y.; Higashi, T.; Nouso, K.; Shiota, T.; Kinugasa, N.; Yoshida, K.; Uematsu, S.; Nakatsukasa, H.; Nishimura, Y.; Tsuji, T. Cathepsin B in the Growth of Colorectal Cancer: Increased Activity of Cathepsin B in Human Colorectal Cancer. *Acta Med. Okayama* **1996**, *50*, 305−311.
(21) Sloane, B. F.; Yan, S.; Podgorski, I.; Linebaugh, B. E.; Cher, M. L.; Mai, J.; Cavallo-Medved, D.; Sameni, M.; Dosescu, J.; Moin, K. Cathepsin B and Tumor Proteolysis: Contribution of the Tumor Microenvironment. *Semin. Cancer Biol.* **2005**, *15*, 149−157.
(22) Podgorski, I.; Sloane, B. F. Cathepsin B and Its Role in Cancer Progression. *Biochem. Soc. Symp.* **2003**, *70*, 263−276.
(23) Premzl, A.; Turk, V.; Kos, J. Intracellular Proteolytic Activity of Cathepsin B Is Associated with Capillary-like Tube Formation by Endothelial Cells in Vitro. *J. Cell. Biochem.* **2006**, *97*, 1230−1240.
(24) Lim, I. T.; Meroueh, S. O.; Lee, M.; Heeg, M. J.; Mobashery, S. Strategy in Inhibition of Cathepsin B, a Target in Tumor Invasion and Metastasis. *J. Am. Chem. Soc.* **2004**, *126*, 10271−10277.
(25) Leto, G.; Pizzolanti, G.; Tumminello, F. M.; Gebbia, N. Effects of E-64 (Cysteine Proteinase Inhibitor) and Pepstatin (Aspartyl Proteinase Inhibitor) on Metastasis Formation in Mice with Mammary and Ovarian Tumors. *In Vivo* **1994**, *8*, 231−236.
(26) Navab, R.; Mort, J. S.; Brodt, P. Inhibition of Carcinoma Cell Invasion and Liver Metastases Formation by the Cysteine Proteinase Inhibitor E-64. *Clin. Exp. Metastasis* **1997**, *15*, 121−129.
(27) Redwood, S. M.; Liu, B.; Weiss, R.; Hodge, D.; Droller, M. J. Abrogation of the Invasion of Human Bladder Tumor Cells by Using Protease Inhibitors. *Cancer* **1991**, *69*, 1212−1219.
(28) Falgueyret, J. P.; Oballa, R. M.; Okamoto, O.; Wesolowski, G.; Aubin, Y.; Rydzewski, R. M.; Prasit, P.; Riendeau, D.; Rodan, S. B.; Percival, M. D. Novel, Nonpeptidic Cyanamides as Potent and Reversible Inhibitors of Human Cathepsins K and L. *J. Med. Chem.* **2001**, *44*, 94−104.
(29) Beynon, R. J.; Salvesen, G. *Proteolytic Enzymes: A Practical Approach*; Beynon, R. J., Bond, J. S., Eds.; IRL Press: Oxford, England, 1989.
(30) Otto, H. H.; Schimeister, T. Cysteine Proteases and Their Inhibitors. *Chem. Rev.* **1997**, *97*, 133−171.
(31) Baici, A.; Gyger-Marazzi, M. The Slow, Tight-Binding Inhibition of Cathepsin B by Leupeptin. A Hysteretic Effect. *Eur. J. Biochem.* **1982**, *129*, 33−41.
(32) Barrett, A. J.; Kembhavi, A. A.; Brown, M. A.; Kirschke, H.; Knight, C. G.; Tamai, M.; Hanada, K. L-*trans*-Epoxysuccinyl-leucylamido-(4-guanidino)butane (E-64) and Its Analogues as Inhibitors of Cysteine Proteinases Including Cathepsins B, H and L. *Biochem. J.* **1982**, *201*, 189−198.
(33) Murata, M.; Miyashita, S.; Yokoo, C.; Tamai, M.; Hanada, K.; Hatayama, K.; Towatari, T.; Nikawa, T.; Katunuma, N. Novel Epoxysuccinyl Peptides. Selective Inhibitors of Cathepsin B, in Vitro. *FEBS Lett.* **1991**, *280*, 307−310.
(34) Turk, D.; Podobnik, T.; Popovic, T.; Katunuma, N.; Bode, W.; Huber, R.; Turk, V. Crystal Structure of Cathepsin B Inhibited with CA030 at 2.0 Å Resolution: A Basis for the Design of Specific Epoxysuccinyl Inhibitors. *Biochemistry* **1995**, *34*, 4791−4797.
(35) Yamamoto, A.; Hara, T.; Tomoo, K.; Ishida, T.; Fujii, T.; Hata, Y.; Murata, M.; Kitamura, K. Binding Mode of CA074, a Specific Irreversible Inhibitor, to Bovine Cathepsin B As Determined by X-ray Crystal Analysis of the Complex. *J. Biochem.* **1997**, *121*, 974−977.
(36) Stern, I.; Schaschke, N.; Moroder, L.; Turk, D. Crystal Structure of NS-134 in Complex with Bovine Cathepsin B: A Two-Headed Epoxysuccinyl Inhibitor Extends along the Entire Active-Site Cleft. *J. Biochem.* **2004**, *381*, 511−517.
(37) Tam, T. F.; Leung-Tong, R.; Li, W.; Spino, M.; Karimian, K. Medicinal Chemistry and Properties of 1,2,4-Thiadiazoles. *Mini-Rev. Med. Chem.* **2005**, *5*, 367−379.
(38) Leung-Tong, R.; Wodzinska, J.; Li, W.; Lowrie, J.; Kukreja, R.; Desilets, D.; Karimian, K.; Tam, T. F. 1,2,4-Thiadiazole: A Novel Cathepsin B Inhibitor. *Bioorg. Med. Chem.* **2003**, *11*, 5529−5537.
(39) Mort, J. S.; Buttle, D. J. Molecules in Focus: Cathepsin B. *Int. J. Biochem. Cell Biol.* **1997**, *29*, 715−720.
(40) Quraishi, O.; Nagler, D. K.; Fox, T.; Sivaraman, J.; Cygler, M.; Mort, J. S.; Storer, A. C. The Occluding Loop in Cathepsin B Defines the pH Dependence of Inhibition by Its Propeptide. *Biochemistry* **1999**, *38*, 5017−5023.
(41) Maresca, K. P.; Femia, F. J.; Babich, J. W.; Zubieta, J. Expansion of the "3 + 1" Concept of Oxorhenium-Thiolate Chemistry to Cationic and Binuclear Complexes. *Inorg. Chem. Commun.* **1998**, *1*, 209−212.
(42) Papadopoulos, M. S.; Pirmettis, I. C.; Pelecanou, M.; Raptopoulou, C. P.; Terzis, A.; Stassinopoulou, C. I.; Chiotellis, E. *Syn*−*Anti* Isomerism in a Mixed-Ligand Oxorhenium Complex, ReO[SN(R)S][S]. *Inorg. Chem.* **1996**, *35*, 7377−7383.
(43) Spies, H.; Fietz, T.; Pietzsch, H.-J.; Johansen, B.; Leibnitz, P.; Reck, G.; Scheller, D.; Klostermann, K. Neutral Oxorhenium(V) Complexes with Tridentate Dithiolates and Monodentate Alkane- or Arenethiolate Coligands. *J. Chem. Soc., Dalton Trans.* **1995**, *13*, 2277−2280.
(44) Femia, F. J.; Chen, X.; Maresca, K. P.; Shoup, T. M.; Babich, J. W.; Zubieta, J. Synthesis and Characterization of Complexes of the $\{ReO\}^{3+}$ Core with SNS and S Donor Ligands. *Inorg. Chim. Acta* **2000**, *306*, 30−37.
(45) Papadopoulos, M. S.; Tsoukalas, C.; Pirmettis, I. C.; Nock, B. A.; Maina, T.; Abedin, Z.; Raptopoulou, C. P.; Terzis, A.; Chiotellis, E. Synthesis and Characterization of Five-Coordinate Rhenium(V) and Techentium(V) Mixed Ligand Bifunctional Complexes Carrying the SNS/S or the SNN/S Donor Atom Set. Crystal Structure of ReO{$[(C_2H_5)_2NCH_2CH_2N(CH_2CH_2S)_2](p\text{-}H_2N\text{-}PhS)$} and ReO{$[(CH_2)_4NCH_2CH_2NCH_2CH_2S](p\text{-}H_2N\text{-}PhS)$}. *Inorg. Chim. Acta* **1999**, *285*, 97−106.
(46) Nock, B. A.; Maina, T.; Yannoukakos, D.; Pirmettis, I. C.; Papadopoulos, M. S.; Chiotellis, E. Glutathione-Mediated Metabolism of Technetium-99m SNS/S Mixed Ligand Complexes: A Proposed Mechanism of Brain Retention. *J. Med. Chem.* **1999**, *42*, 1066−1075.
(47) Pelecanou, M.; Pirmettis, I. C.; Nock, B. A.; Papadopoulos, M. S.; Chiotellis, E.; Stassinopoulou, C. I. Interaction of [ReO(SNS)(S)] and [^{99m}TcO(SNS)(S)] Mixed Ligand Complexes with Glutathione: Isolation and Characterization of the Product. *Inorg. Chim. Acta* **1998**, *281*, 148−152.
(48) Nock, B. A.; Maina, T.; Tsortos, A.; Pelecanou, M.; Raptopoulou, C. P.; Papadopoulos, M. S.; Pietzsch, H.-J.; Stassinopoulou, C. I.; Terzis, A.; Spies, H.; Nounesis, G.; Chiotellis, E. Glutathione Interaction with SNS/S Mixed-Ligand Complexes of Oxorhenium(V): Kinetic Aspects and Characterization of the Products. *Inorg. Chem.* **2000**, *39*, 4433−4441.
(49) Baird, I. R.; Mosi, R.; Olsen, M.; Cameron, B. R.; Fricker, S.; Skerlj, R. "3 + 1" Mixed-Ligand Oxorhenium(V) Complexes and Their Inhibition of the Cysteine Proteases Cathepsin B and Cathepsin K. *Inorg. Chim. Acta* **2006**, *359*, 2736−2750.
(50) Fietz, T.; Leibnitz, P.; Spies, H.; Johansen, B. Synthesis and Reactions of New Oxorhenium(V) Complexes with Re−Halogen Bonds. X-ray Crystal Structure of [(3-benzyl)azapentane-1,5-dithiolato)iodo]-oxorhenium(V). *Polyhedron* **1999**, *18*, 1793−1797.
(51) Fietz, T.; Spies, H.; Pietzsch, H.-J.; Leibnitz, P. Synthesis and Molecular Structure of Chloro(3-thiapentane-1,5-dithiolato)-oxorhenium(V). *Inorg. Chim. Acta* **1995**, *231*, 233−236.
(52) Maresca, K. P.; Femia, F. J.; Bonavia, G. H.; Babich, J. W.; Zubieta, J. Cationic Complexes of the "3 + 1" Oxorhenium-thiolate Family. *Inorg. Chim. Acta* **2000**, *297*, 98−105.
(53) Pirmettis, I. C.; Papadopoulos, M. S.; Mastrostamatis, S. G.; Raptopoulou, C. P.; Terzis, A.; Chiotellis, E. Synthesis and Characterization Of Oxotechnetium(V) Mixed-Ligand Complexes Containing a Tridentate N-Substituted Bis(2-mercaptoethyl)amine and a Monodentate Thiol. *Inorg. Chem.* **1996**, *35*, 1685−1691.
(54) Cunha, R. L. O. R.; Urano, M. E.; Chagas, J. R.; Almeida, P. C.; Bincoletto, C.; Tersariol, I. L. S.; Comasseto, J. V. Tellurium-Based Cysteine Protease Inhibitors: Evaluation of Novel Organotellurium-(IV) Compounds as Inhibitors of Human Cathepsin B. *Bioorg. Med. Chem. Lett.* **2005**, *15*, 755−760.
(55) Chircorian, A.; Barrios, A. M. Inhibition of Lysosomal Cysteine Proteases by Chrysotherapeutic Compounds: A Possible Mechanism for the Antiarthritic Activity of Au(I). *Bioorg. Med. Chem. Lett.* **2004**, *14*, 5113−5116.
(56) Rich, D. L. *Inhibitors of Cysteine Proteinases*; Elsvier Science: Amsterdam, The Netherlands, 1986; pp 153−178.
(57) Kitz, R.; Wilson, I. B. Esters of Methanesulfonic Acid as Irreversible Inhibitors of Acetyl Choline Esterase. *J. Biol. Chem.* **1962**, *237*, 3245−3240.
(58) Cornish-Bowden, A. *Fundamentals of Enzyme Kinetics*; Portland Press: London, U.K., 1995; pp 105−112.
(59) Zechel, D. L.; He, S.; Dupont, C.; Withers, S. G. Identification of Glu-120 as the Catalytic Nucleophile in Streptomyces Lividans Endoglucanase Celb. *Biochem. J.* **1998**, *336*, 139−145.
(60) Varughese, K. I.; Ahmed, F. R.; Carey, P. R.; Hasnain, S.; Huber, C. P.; Storer, A. C. Crystal Structure of a Papain−E-64 Complex. *Biochemistry* **1989**, *28*, 1330−1332.
(61) Matsumoto, I.; Nakagawa, K.; Horiuchi, K. Japanese Patent JP 47017778, 1972.

(62) Rose, D. J.; Maresca, K. P.; Kettler, P. B.; Chang, Y. D.; Sognomomian, V.; Chen, Q.; Abrams, M. J.; Larsen, S. K.; Zubieta, J. Synthesis and Characterization of Rhenium Thiolate Complexes. Crystal and Molecular Structures of $[NBu_4][ReO(H_2O)Br_4)]\cdot 2H_2O$, $[NBu_4][ReOBr_4(OPPh_3)]$, $[ReO(SC_5H_4N)_3]$, $[ReO(OH)(SC_5H_4N\text{-}3,6\text{-}(SiMe_2Bu^t)_2)_2]$, $[Re(N_2COC_6H_5)(SC_5H_4N)Cl(PPh_3)_2]$, and $[Re(PPh_3)(SC_4H_3N_2)_3]$. *Inorg. Chem.* **1996**, *35*, 3548−3558.

(63) Nock, B. A.; Pietzsch, H.-J.; F. T.; Maina, T.; Leibnitz, P.; Spies, H.; Chiotellis, E. Oxorhenium Mixed-Ligand Complexes with the 2,6-Dimercaptomethylpyridine Ligand. Crystal Structure of [2,6-dimercaptomethylpyridinato][*p*-methoxybenzenethiolato]oxorhenium-(V). *Inorg. Chim. Acta* **2000**, *304*, 26−32.

(64) Reich, T.; Bernhard, G.; Nitsche, H.; Spies, H.; Johansen, B. Structural Investigations of Technetium and Rhenium Complexes by EXAFS. 1. Studies on "$n + 1$" Mixed-Ligand Rhenium Complexes. *Forschungszent. Rossendorf, [Ber.] FZR* **1996**, *122*, 141−145.

(65) Fietz, T.; Leibnitz, P. Reactions of Hydroxy-Group Containing "3 + 1" Mixed-Ligand Rhenium(V) Complexes. Part 3. Unexpected Reaction of "3 + 1" Mixed-Ligand Complexes with Thionyl and Acyl Halides and Methyl Iodide. Structural Considerations for a New Modification of Chlorooxo(3-thiapentane-1,5-dithiolato)rhenium(V). *Forschungszent. Rossendorf, [Ber.] FZR* **1997**, Annual Report, 119−123.

(66) Annastassov, V.; Cox, J.; Mosi, R.; Lau, G.; Labrecque, J.; Fricker, S. Cysteine Proteases as a Therapeutic Target: Cloning, Expression and Purification of Cathepsin B and Cathepsin L. Presented at the 85th Canadian Chemistry Society Conference and Exhibition, 2002.

(67) Leatherbarrow, R. Grafit, version 4.09; Erithacus Software: Staines, U.K., 1989.

JM060357Z